Detecting the onset of bifurcations and their precursors from noisy data

Larsson Omberg,[1,2] Kevin Dolan,[1] Alexander Neiman,[1] and Frank Moss[1]
[1]*Center for Neurodynamics, University of Missouri at St. Louis, St. Louis, Missouri 63121*
[2]*Royal Institute of Technology (KTH), Stockholm, Sweden*
(Received 7 October 1999)

We study the problem of the detection of noise-induced precursors of periodic motion instabilities in stochastic dynamical systems. In particular, we concentrate on the period-doubling bifurcation. We have developed a statistical method to detect the onset of bifurcations and their precursors based on the previously established topological recurrence technique.

PACS number(s): 05.40.−a, 05.45.−a, 87.10.+e

I. INTRODUCTION

Nonlinear dynamical systems are extremely sensitive to external perturbations near instabilities. That is because the influence of noise becomes crucial near bifurcation points. The notion of bifurcation in stochastic systems is blurred [1], so that it is difficult to define unambiguously the precise point of bifurcation. For extremely weak noise the bifurcation analysis can be carried out in terms of an effective potential [2,3] or by using cumulant analysis [4,5]. Indeed, noise blurs the whole bifurcation structure of the parameter space of the system and shifts the onset of bifurcation [6,7]. However, another important effect of noise is that it brings forth the noisy precursors of bifurcations. Wiesenfeld [8] has shown that the spectral density of a system observed after a bifurcation point can be visible even before the bifurcation actually occurs if there is noise present. One is thus able to observe a warning indication of the bifurcation in the form of its noisy precursor. Recently it has been shown that the noisy precursors are most pronounced at an optimal noise level [9], demonstrating therefore an effect which is similar to stochastic resonance [10–12].

Observation of noisy precursors might be of great practical importance as a possible indication of the onset of an instability. In particular, recently noisy precursors have been used to make a closed-loop monitoring system for detecting instabilities [13]. Prediction of incipient instabilities might be especially important for biological systems. Besides possible applications in the control of dynamical systems [14,15], observation of the bifurcation behavior allows one to draw qualitative conclusions about the structure of the dynamics of the system. However time series of biological origin are characterized by nonstationarity and are often therefore restricted in length. Because they require long stationary data sets, direct application of measures based on the spectral density estimations can be ineffective and in some cases even useless for nonstationary or heavily noise contaminated signals. In contrast, statistically based topological recurrence methods have recently been shown to effectively detect the signatures of low-dimensional behaviors in data sets from nonstationary, even periodically or transiently stimulated, neural systems [16,17].

In this paper we propose a simple statistical technique to detect dynamical instabilities from the topology of the recurrences in a Poincaré map. Our method is based on a universal structure of this return map in the vicinity of local bifurcations of periodic solutions. In particular we concentrate on the period doubling bifurcations that are typical for a wide variety of dynamical systems. We look for occurrences of a certain pattern in a time series which is a universal signature for a suspected dynamical instability buried in noise and then compare the result with a surrogate data set to determine the statistical significance of the result [18]. Therefore, this method is closely akin to that for detecting unstable periodic orbits (UPO's) [19–21] and can be generalized for the detection of precursors of other local bifurcations. This paper is organized as follows. In Sec. II, we briefly discuss the noisy precursor of a period-doubling instability, using the examples of the logistic map and the Rössler system. In Sec. III, we introduce the method and present some results of its applications. In Sec. IV, we compare the method with the traditional spectral analysis. The discussion is presented in Sec. V

II. NOISY PRECURSOR OF THE PERIOD DOUBLING BIFURCATION

We illustrate the noisy precursor of the period-doubling bifurcation first using the Rössler system [22]. With additive white noise the system is governed by the three-dimensional stochastic differential equations

$$\dot{x} = -(y+z) + \sqrt{2D}\xi_1(t), \quad \dot{y} = x + ay + \sqrt{2D}\xi_2(t), \quad \dot{z} = b + z(x-c) + \sqrt{2D}\xi_3(t), \tag{1}$$

where a, b, and c are the parameters, D is the intensity of the statistically independent white noises $\xi_i(t)$. In the absence of noise ($D=0$), and with the parameter values $a=b=0.2$, the first period-doubling bifurcation occurs at $c=c_1\approx 2.835$. For $c<c_1$ the power spectrum of the noise-free system consists of δ peaks at a basic frequency ω_0 and its harmonics. Beyond the bifurcation parameter value, $c>c_1$ the power spectrum of the system possesses also δ peaks at subharmonics of a base frequency, $\omega_0 \pm \omega_0/2$.

With noise switched on, the precursors of period-doubling become visible even before the bifurcation. In Fig. 1, we show the power spectra of the x coordinate of the Rössler system for different noise intensities. In the absence of noise the spectral density possesses a peak at $\omega_0\approx 1.09$, which

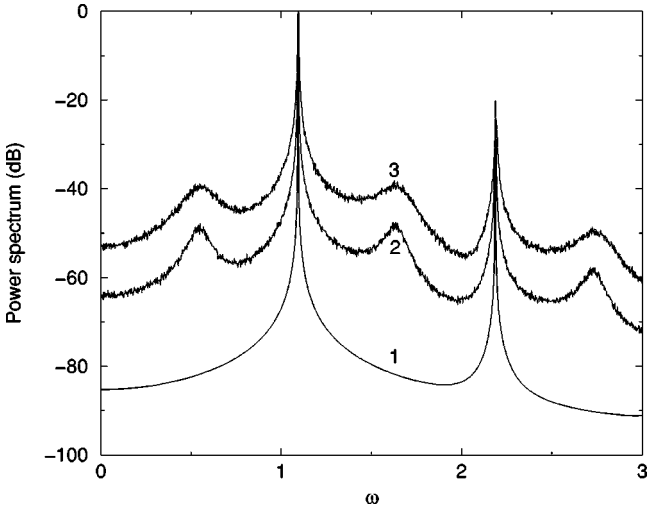

FIG. 1. Power spectrum of the x coordinate of the Rössler system for $c=2.5$ and different values of noise intensities. The numbers near the plots correspond to: $D=0.0$ (1), $D=0.001$ (2), $D=0.01$ (3).

corresponds to the natural frequency of the stable limit cycle. The noise-induced precursor appears in the form of broadband peaks at the subharmonics $\omega_{\mp}=\omega_0\mp\omega_0/2$.

Let us consider the control parameter region preceding the period doubling bifurcation in more detail. For this purpose we introduce a Poincaré return map, $\tau_{n+1}=f(\tau_n)$, that is we consider a sequence of time intervals τ_n between consecutive intersections of a phase trajectory with a transversal surface in the phase space. In neuronal electrophysiology the Poincaré return map corresponds to the intervals between action potentials, or spikes, of the membrane potential (or simply interspike intervals). A stable limit cycle corresponds to the existence of a stable fixed point in the Poincaré return map. The stability of a limit cycle is determined by its characteristic or Floquet multipliers which are the eigenvalues of the corresponding linearized Poincaré map [23]. Stable limit cycles possess multipliers whose absolute values are less than 1. The birth of a limit cycle corresponds to the situation when one of the multipliers crosses to $+1$ while the period-doubling bifurcation corresponds to the situation when one of the multipliers crosses -1. In the absence of noise the power spectrum calculated from the discrete time series of the return times possesses a δ peak at $\omega_0=0$ (or 2π) for the stable period-1 cycle. For stable cycles of period $2^k(k>1)$ the power spectrum has peaks at ''subharmonic frequencies'' $\omega_k=(2m+1)\pi/2^{k-1}$ $(m=0,1,2,\ldots)$.

For parameter values preceding the period doubling bifurcation the real part of the largest (by absolute value) multiplier changes from positive to negative and finally reaches the value -1 at the point of period doubling. The qualitative changes of the dynamics of the Poincaré return map can be visualized using Lamerey diagrams [24], also called the cobweb construction [23]. These diagrams show geometrically how a perturbation approaches the fixed point. In Fig. 2 we show numerically obtained Lamerey diagrams [24] for the Poincaré return map of the Rössler system for two parameter values: when the real part of the largest multiplier, ρ, is positive (a) and negative (b). Although in both cases the limit cycle is stable (as is the corresponding fixed point in the

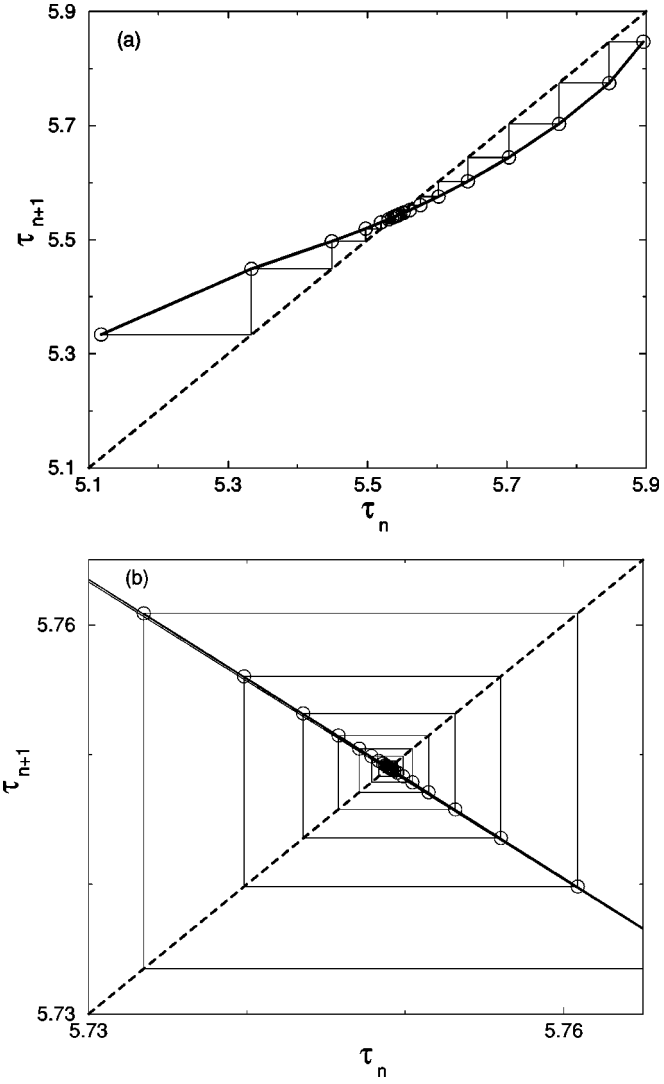

FIG. 2. Poincaré return maps $\tau_{n+1}=f(\tau_n)$ of the Rössler system for different values of the control parameter are shown as Lamerey diagrams: (a) $c=1.0$, $\rho>0$; (b) $c=2.5$, $\rho<0$.

return map), the structure of approaches to the fixed point is qualitatively different. In the case $\rho>0$ we have a Lamerey staircase [Fig. 2(a)], while for the negative multiplier the return map is represented by the Lamerey spiral [Fig. 2(b)]. The qualitative change in the behavior of the system in the neighborhood of the stable fixed point occurs when the multiplier crosses zero.

Let us linearize the return map near the stable fixed point. Denote the fixed point as τ_0, and introduce a small deviation from it as $\theta_n=\tau_n-\tau_0$. Then for a weak noise the linearized map can be written as

$$\theta_{n+1}=\rho\theta_n+\xi_n, \tag{2}$$

where ξ_n is a Gaussian noise with the power spectrum $G_{\xi}(\omega)$, and $\rho=df(\tau)/d\tau|_{\tau=\tau_0}$ is the multiplier of the fixed point. We require that $|\rho|<1$, e.g., the fixed point is stable. The power spectrum $G_{\theta}(\omega)$ of this linear stochastic map can be easily calculated [4] providing

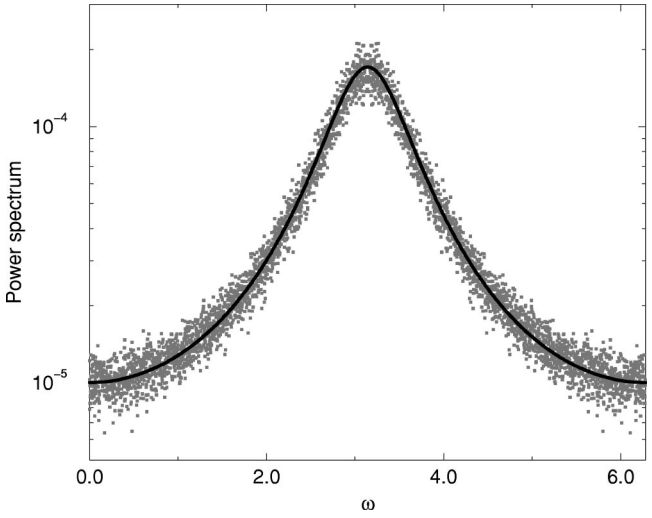

FIG. 3. Power spectrum calculated from the return map of the Rössler system with $c=2.5$ and $D=0.01$ is shown by gray dots. The solid line represents the analytic estimate from Eq. (3) where the noise spectrum $G_{\xi}(\omega)$ was taken as a constant.

$$G_{\theta}(\omega)=\frac{G_{\xi}(\omega)}{1-2\rho\cos\omega+\rho^{2}}. \tag{3}$$

In the absence of noise the power spectrum has indeed a δ-peak at $\omega_0=0$. With noise and for positive values of multipliers the power spectrum (3) has a broad peak at the basic frequency $\omega=0$ (or $\omega=2\pi$). Otherwise, once ρ is negative the peak in the power spectrum is centered at $\omega=\pi$, that is, noise gives rise to the fact that the power spectrum reflects a structure that is typical for a fixed point of period 2, long before the occurrence of the bifurcation point in the appropriate deterministic case. In particular, for the Rössler system the largest multiplier crosses zero at $c=c_0=1.57$, while the period-doubling bifurcation occurs at $c=c_1\approx 2.835$. The power spectrum of the Poincaré return map obtained numerically from the stochastic Rössler system is shown in Fig. 3 and is in very good agreement with the theoretical estimation of Eq. (3). This analysis is valid for the limit of weak noise. The cases of intermediate and large noise have been considered in terms of the power spectrum in Ref. 9.

Theoretically, the noisy precursor should appear right at the transition point $\rho=0$. However, according to the theory of Wiesenfeld [8] the height, h, of the noise-induced peaks and their width, $\Delta\omega$, scale with critical parameter $\epsilon=c_1-c$ as $h\propto\epsilon^{-2}$ and $\Delta\omega\propto\epsilon$. Thus the further we are from the period doubling bifurcation, the less pronounced is the noise-induced peak in the power spectrum. From the point of view of the return map, the larger (by absolute value) the multiplier, the more turns there are in the Lamerey spiral, and consequently the higher is the noise-induced peak in the power spectrum. At large noise, however, this peak may become indistinguishable. Therefore, in experimental situations for which the dynamics are inherently noisy, for example, those typical of biology, it is difficult to detect an incipient instability far from the actual bifurcation if one is using the power spectrum alone as an indicator.

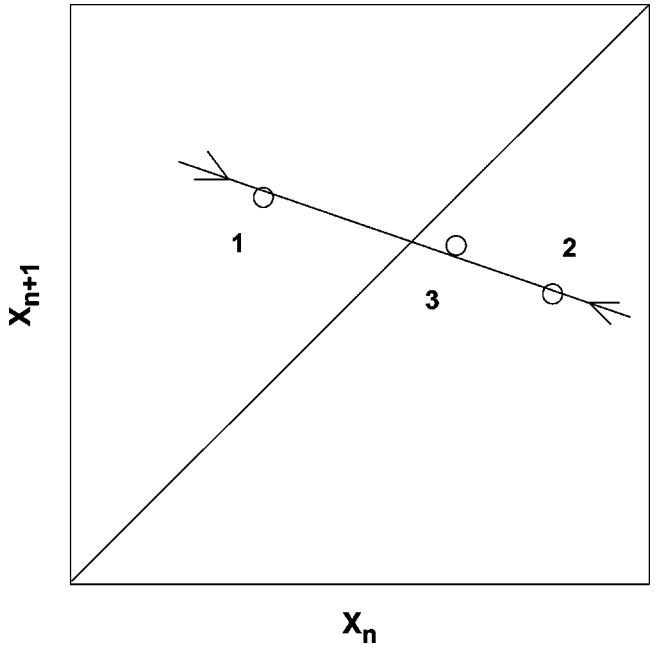

FIG. 4. The structure of an encounter. There are three points approaching the fixed point. The points are scattered along a line with negative slope.

III. DETECTING PRECURSORS USING TOPOLOGICAL METHODS

Here we develop a statistical method based on the qualitative properties of the behavior of the return map shown in Fig. 2. One such property is the slope of the approaching trajectory, which shows a trademark negative value prior to a period doubling bifurcation. This trademark can be detected by looking for consecutive points approaching the fixed point along a line whose slope is negative. The slope is determined using a linear regression of the points, and directly corresponds to the value of the multiplier. Specifically, the pattern looked for has two criteria:

(i) Three points on the return map fall such that their perpendicular distances to the 45° line become consecutively smaller.

(ii) The three points lie approximately along a line of negative slope.

For a geometrical description of these criteria see Fig. 4. The pattern looked for is a modification of the topological recurrence method used to search for unstable periodic orbits (see Refs. [19–21], [16], and [17]). Such patterns are called *encounters* when they are located in a time series. This pattern will be found with some probability in any system, even purely stochastic systems, and systems with fixed points with positive multipliers. In the case of systems with negative multipliers, it should occur with much greater frequency then one would expect from mere chance. To obtain a statistical measure of the number of encounters with the above mentioned pattern, the number of encounters N was compared to the number of encounters found in surrogate data files, N_s. The surrogate files were created by randomly shuffling the original time series. Taking M different realizations of surrogates to determine an average $\langle N_s\rangle$ and standard deviation σ, we use the following formula,

$$Q = \frac{N - \langle N_s \rangle}{\sigma}, \tag{4}$$

where Q is a measure, in units of standard deviations, between the searched for pattern and the surrogate findings. In a completely random data file, the number of encounters found will be a binomially distributed random variable. This means that as long as the number of encounters found on average in the surrogates is greater then about 20, the distribution will be Gaussian. The statistic Q can thus be used to determine the probability that the data file could have come from the same distribution as the surrogates. A value of Q larger than positive 3 therefore corresponds to a chance of less than 1% that the detected encounters are the result of pure chance [25]. A large negative value means that the pattern is suppressed in the data, possibly indicating some other type of dynamics. With respect to period doubling bifurcations, when the multiplier is positive the approach toward the fixed point is favored along a positive slope, and hence encounters with the pattern defined above may be suppressed. Typically Q is negative for positive multipliers, and becomes positive for negative multipliers, growing larger as the multiplier becomes more negative.

To demonstrate this we applied the analysis to two systems, the logistic map and the previously described Rössler system. The logistic map is written as:

$$x_{n+1} = a x_n (1 - x_n) + \sqrt{2D}\xi_n, \tag{5}$$

where a is the bifurcation parameter, D is the intensity of the white noise ξ_n. In the noiseless case, $D=0$, the multiplier crosses zero for $a=2$ and becomes smaller than -1 for $a > 3$ which is the point where the system bifurcates to a stable period 2 orbit. The multiplier for this orbit remains positive until $a \approx 3.235$ where it crosses zero and grows towards negative values until $a \approx 3.4986$ where the period two orbit becomes unstable and the system again bifurcates. Using the topological search on the first return map we were able to detect significant positive statistic $Q > 3.0$ well before the first bifurcation [Fig. 5(a)].

We can also expand our analysis to period two orbits, by using the second return map, that is looking at every other point in the data set, first $x_1, x_3, \ldots, x_{n-1}$, then $x_2, x_4, \ldots, x_n$. Encounters with the period two orbit will appear both in the first and second pass as a series of points converging towards the 45° line. The multiplier associated with the period two orbit is still given by the slope of the converging points on the return map, so by applying the same algorithm to the period two return map, we are able to detect the precursors in the period two region as well [Fig. 5(b)].

As already discussed, the Rössler system goes through a bifurcation sequence similar to that of the logistic map. The first bifurcation occurs at $c \approx 2.835$, and the second bifurcation at $c \approx 3.8376$. Just as for the logistic map the first return map was studied in the period one region and the second return map in the period 2 region. The Q statistic grows as the multiplier becomes more negative, and once again becomes significantly positive well before the bifurcation occurs, as shown in Fig. 6.

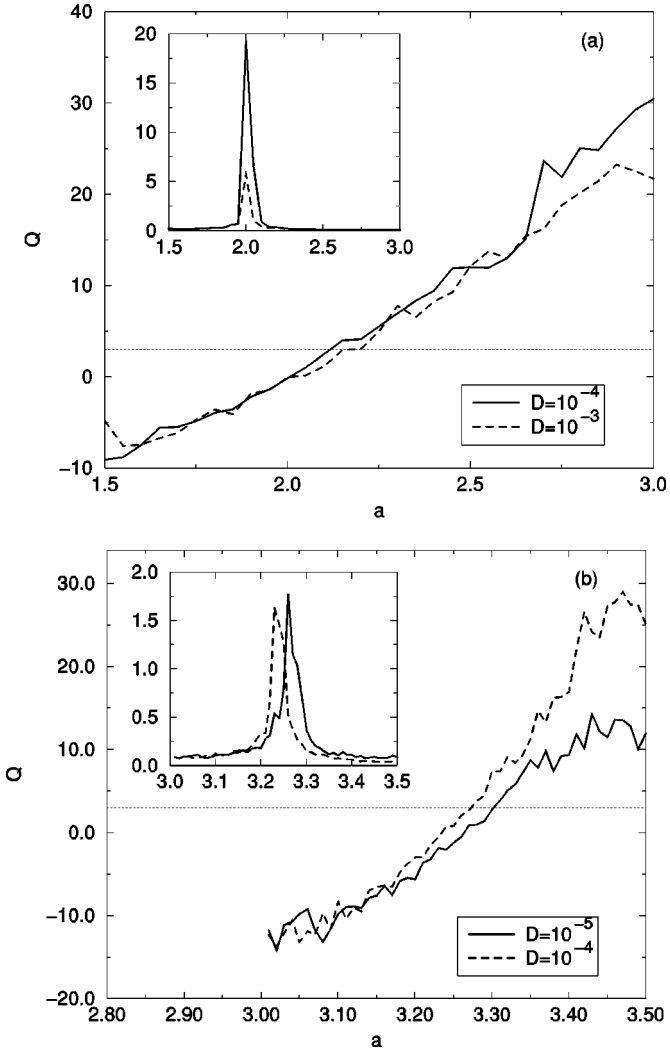

FIG. 5. Q statistic vs bifurcation parameter a for the logistic map (a) prior to first bifurcation ($a=3$) (b) nearing second bifurcation ($a \approx 3.499$). At each value of a, 50 000 data points were analyzed using Eq. (4) to calculate Q. Remember that according to the statistics assumed a value of Q above 3 is considered a significant finding. The insets show $|1/Q|$ versus a, which give an indication of the zero crossings. Note how closely the peak corresponds to the theoretical values of the noiseless system.

As discussed above Q will have a large negative value when the pattern is suppressed as is the case when the multiplier is positive and the approach is along a positive slope. Furthermore the parameter seems to grow as the multiplier becomes more negative, which means there has to be a point of zero statistic. By plotting $|1/Q|$ versus the bifurcation parameter, an approximate value for this crossing can be obtained as a sharp peak in the plot, see insets of Figs. 5 and 6. Not surprisingly these peaks fall very close to the zero crossings of the multipliers: $a=2$ and $a \approx 3.235$ for the logistic map and $c \approx 1.57$ and $c \approx 3.274$ for the Rössler system.

Although, as is well known [6], noise shifts bifurcation points, it should be noted from Figs. 5 and 6 that even though the noise amplitude varies by a factor of 10, the statistic Q, taken at the 99% confidence level, is virtually uneffected. Therefore, this method is very robust to the influence of noise.

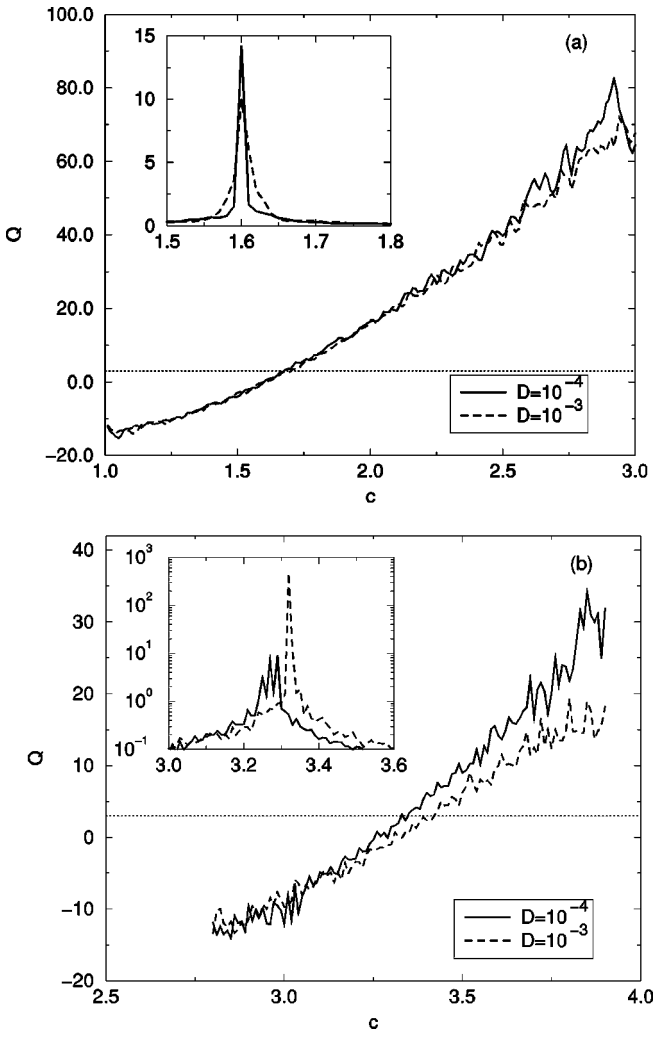

FIG. 6. Q statistic for the Rössler system as function of c: (a) approaching first bifurcation ($c \approx 2.835$) and (b) approaching the second bifurcation ($c \approx 3.8376$). The graph is a running average over three points of c where each Q value was calculated from 50 000 data points. For a significance level of 99% the Q value has to surpass 3. The insets show $1/Q$ versus the bifurcation parameter, notice how again the peaks fall close to the multiplier zero crossings of 1.57 and 3.274.

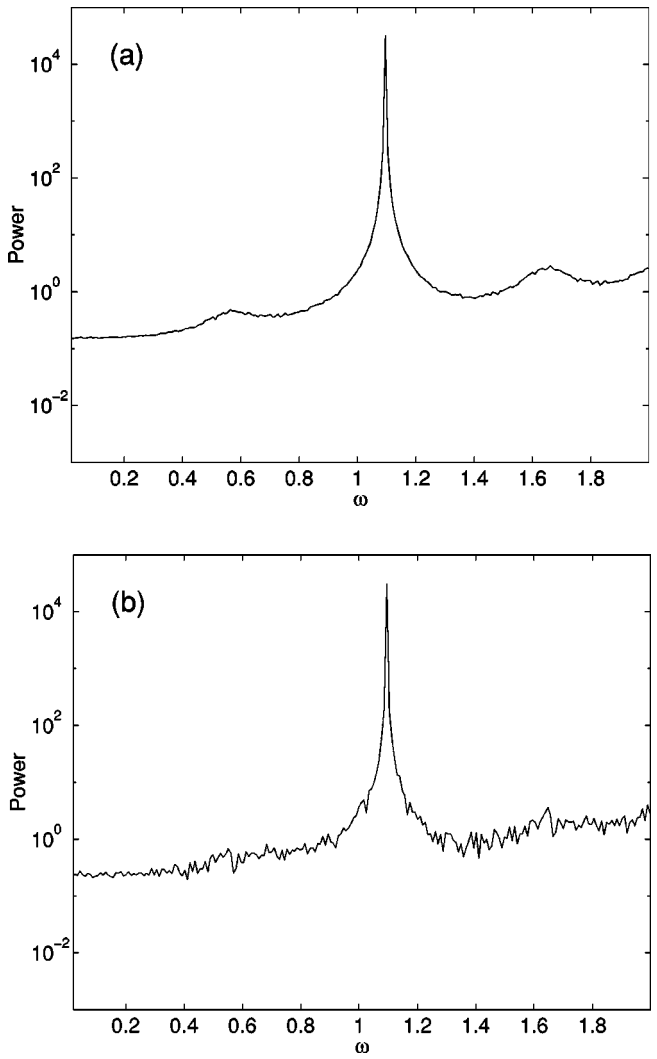

FIG. 7. Power Spectrum of Rössler system with $D = 0.001$ and $c = 2.3$ obtained from (a) a long data series consisting of 32 768 Poincaré crossings and (b) a short data series of 1024 Poincaré crossings. Notice that the precursors appear at $\omega_0 \pm \omega_0/2$ in (a), but they cannot be observed in (b). Both cases show strong statistics, $Q = 20.1$ and $Q = 5.6$, respectively.

IV. COMPARING TOPOLOGICAL METHODS TO POWER SPECTRAL ANALYSIS

As stated in Sec. II the length of the time series is a limiting factor when using the power spectra to detect precursors. The topological method presented is less sensitive to the length of the data set. Since the above analysis is based on finding specific events in the data instead of averaging over the whole data set, as the power spectrum method does, it works like a filter on the data reducing the noise by only taking into account the data that actually fits the pattern.

To show how the method is apt to work with short data sets, power spectra were calculated for the Rössler system far from the bifurcation ($c = 2.3$) using data sets of different lengths. The length of the data sets were defined by the number of crossings of the Poincaré section. The longer data set shows the appearance of precursors, while in shorter data sets these are obscured by the noise in the system as shown in Fig. 7. In contrast, our method is free from this limitation on the data set length and yields strongly positive statistics for both time series, that is for 1024 points, $Q = 5.6$, and for 32768 points, $Q = 20.1$.

The way the statistic Q scales with file length can be undrestood by looking at how it is calculated [Eq. (4)]. Assuming that the system being analyzed really does possess the type of dynamics we are looking for, the number of encounters N found in the file should be proportional to the length of the file L. Furthermore, we can think of a long surrogate file as being several smaller surrogate files placed end to end. The random variable $\langle N_s \rangle$ is thus simply the sum of several independent random variables, so $\langle N_s \rangle$ and σ are proportional to L and $\sqrt{L}$ respectively. We can therefore conclude that $Q \propto \sqrt{L}$, which is well supported by the our analysis applied to the Rössler system as shown in Fig. 8.

This is in contrast to the case of detecting a signal in a noisy background using the power spectra, where the signal to noise ratio varies linearly with file length.

The ability to operate on very short data files is of great

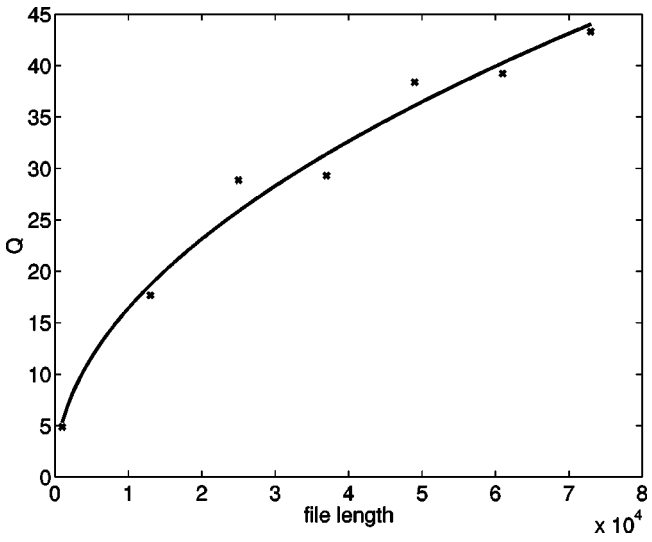

FIG. 8. The dependence of Q versus the length of the sequence of the Poincaré return times for the Rössler system. The crosses correspond to the results of our analysis, while the solid line represents the square root law (see text). The parameters are the same as in the previous figure.

importance in biophysics research, since long data files are often impossible to obtain. This topological method can also be very useful for analysis of non-stationary systems. By looking at small intervals over which the system is approximately stationary, one could use these methods to determine when the system is about to undergo a bifurcation. The topological method is ideally suited to this type of analysis, wheras the power spectra method is significantly limited by the short data files.

V. DISCUSSION

The topological method described in this paper provides an alternative to power spectral analysis for detecting the onset of dynamical instabilities. The ability of this method to operate on very short and noisy data files creates the opportunity to apply the detection of noisy precursors to systems that could not previously be analyzed. An example of where this method could open up new doors is in experimental biology, in particular in the electrophysiology of neural systems. These systems are invariably noisy, and therefore data sets from them are often severely limited in length due to nonstationarity. Another possibility is to apply the method to nonstationary systems where the data can be broken down into smaller segments with almost stationary dynamics. An example is the possibility to predict the tonic-to-bursting bifurcations in neural firing patterns of various sensory neural systems before they actually occur.

The computational simplicity of our method also presents interesting opportunities for real time analysis. This could be useful in the control of dynamical systems where one wants to predict an instability before it happens.

ACKNOWLEDGMENTS

We are grateful to M. L. Spano, H. A. Braun, and M. Huber for stimulating discussions and essential insights. This work was supported by the U.S. Office of Naval Research, The Fetzer Institute, and the Department of Energy.

[1] L. Arnold, *Random Dynamical Systems* (Springer, Berlin, 1998).
[2] M. I. Freidlin and A. D. Wentzell, *Random Perturbations of Dynamical Systems* (Springer, Berlin, 1984).
[3] R. Graham, in *Noise in Nonlinear Dynamical Systems*, edited by F. Moss and P. V. E. McClintock (Cambridge University Press, Cambridge, England, 1989).
[4] A. Neiman, V. Anishchenko, and J. Kurths, Phys. Rev. E **49**, 3801 (1994).
[5] A. Neiman, U. Feudel, and J. Kurths, J. Phys. A **28**, 2471 (1995).
[6] L. Fronzoni, R. Mannella, P. V. E. McClintock, and F. Moss, Phys. Rev. A **36**, 834 (1987).
[7] C. Meunier and A. D. Verga, J. Stat. Phys. **50**, 345 (1988).
[8] K. Wiesenfeld, J. Stat. Phys. **38**, 1071 (1985).
[9] A. Neiman, P. I. Saparin, and L. Stone, Phys. Rev. E **56**, 270 (1997).
[10] R. Benzi, A. Sutera, and A. Vulpiani, J. Phys. A **14**, L453 (1981).
[11] R. Benzi, G. Parisi, A. Sutera, and A. Vulpiani, Tellus **34**, 10 (1982).
[12] K. Wiesenfeld and F. Moss, Nature (London) **373**, 33 (1995).
[13] T. Kim and E. H. Abed, IEEE Trans. Circuits Syst., I (in press).
[14] W. L. Ditto, M. L. Spano, and J. F. Lindner, Physica D **86**, 198 (1995).
[15] A. Garfinkle, M. L. Spano, W. L. Ditto, and J. N. Weiss, Science **257**, 1230 (1992).
[16] H. A. Braun, K. Schäfer, K. Voigt, R. Peters, F. Bretschneider, X. Pei, L. Wilkens, and F. Moss, J. Comput. Neurosci. **4**, 335 (1997).
[17] H. A. Braun, M. Dewald, K. Schäfer, K. Voigt, X. Pei, K. Dolan, and F. Moss, J. Comput. Neurosci. **7**, 17 (1999).
[18] K. Dolan, W. Witt, M. L. Spano, A. Neiman, and F. Moss, Phys. Rev. E **59**, 5235 (1999).
[19] D. Pierson and F. Moss, Phys. Rev. Lett. **75**, 2124 (1995).
[20] X. Pei and F. Moss, Nature (London) **379**, 618 (1996).
[21] X. Pei and F. Moss, Int. J. Neural Syst. **7**, 429 (1996).
[22] O. E. Rössler, Phys. Lett. A **57**, 397 (1976).
[23] S. H. Strogatz, *Nonlinear Dynamics and Chaos* (Addison-Wesley, NY, 1994).
[24] L. P. Shilnikov, A. L. Shilnikov, D. V. Turaev, and L. O. Chua, *Methods of Qualitative Theory in Nonlinear Dynamics. Part I* (World Scientific, Singapore, 1998).
[25] P. R. Bevington, in *Data Reduction and Error Analysis* (McGraw-Hill, New York, 1969), pp. 48–49.